Eur. Phys. J. D **14**, 27–31 (2001)

THE EUROPEAN PHYSICAL JOURNAL D

EDP Sciences

Collision-time asymmetry of the ^{114}Cd 326.1 nm line perturbed by Ar

A. Bielski, D. Lisak, and R.S. Trawiński[a]

Institute of Physics, Nicholas Copernicus University, Grudziądzka 5/7, 87–100 Toruń, Poland

Received 19 July 2000

Abstract. Using a laser-induced fluorescence method a detailed analysis of profiles of the ^{114}Cd 326.1 nm line perturbed by argon was performed which revealed deviations from the ordinary Voigt profile. These deviations are shown to be consistent with fits of experimental profiles to an asymmetric Voigt profile. Coefficients of the pressure broadening, shift and collision-time asymmetry are determined and compared with those calculated in the adiabatic approximation for different interaction potentials.

PACS. 32.70.-n Intensities and shapes of atomic spectral lines – 33.70.-w Intensities and shapes of molecular spectral lines and bands – 34.20.-b Interatomic and intermolecular potentials and forces, potential energy surfaces for collisions

1 Introduction

In experiments on pressure effects on atomic spectra one usually assumes that at low densities of perturbing atoms their collisions with emitting atoms give rise to a Lorentzian profile which is symmetric with respect to the position of the peak of the line. The use of Lorentzian profiles for the interpretation of the experimental data is justified for isolated lines if the collision duration can be neglected [1–3]. This means that in such a treatment the collisions are assumed to be effectively instantaneous. If the finite duration of the collisions is taken into account, the first-order correction term to the Lorentzian profile appears to have a dispersion form the intensity of which is proportional to the collision-duration time [2–10]. For some atomic systems this dispersion-shaped correction may be important even for frequencies located not far away from the line core, *i.e.* in the so-called near wing region. In general, it causes that the resulting line profile in this region becomes asymmetric and this type of asymmetry is referred to as the collision-time asymmetry. It should be noted that the collision-time asymmetry was measured by now only for a few spectral lines of some elements perturbed by rare gases (see *e.g.* [11] and references therein).

In a recent paper [12] we reported results of detailed studies of the shape of the 326.1 nm ^{114}Cd line perturbed by xenon which were performed using a laser-induced fluorescence (LIF) technique. A good signal to noise ratio and negligible instrumental profile enabled us to fit the line shapes in considerable detail and record deviations from the ordinary Voigt profile. In the course of our systematic study on pressure effects on Cd 326.1 nm line, in this paper we report the results of measurements of the pressure broadening, shift and asymmetry of this line perturbed by argon.

The experimental studies of pressure broadening and shift of the Cd 326.1 nm line perturbed by Ar were performed by Dietz *et al.* [13] and in this laboratory [16] where the pressure broadening and shift of the ^{114}Cd 326.1 nm ($5^1S_0-5^3P_1$) intercombination line perturbed by Ar were studied by means of classical emission spectroscopy using a pressure-scanned Fabry-Perot interferometer. It should be noted that due to the weakness of the fluorescence signal and small transmission of the Fabry-Perot interferometer, being its inherent feature, such line shape measurements were possible only for the perturbing gas pressures less than 100 torr at room temperature. Moreover, our earlier measurements could be affected by systematic error due to incomplete knowledge of the instrumental function of a real Fabry-Perot (FPI) interferometer. Our experimental tests and numerical simulations showed that for the real FPI it was practically impossible to observe the collision-time asymmetry since this rather small effect is totally obscured by a periodic instrumental function of FPI. The above limitation and rather low – especially for higher pressures – signal to noise ratio did not allowed us in our previous work [16] to register and analyze the collision-time asymmetry for the Cd–Ar system. We have therefore thought it necessary to carry out new measurements of the shapes of the Cd 326.1 nm line perturbed by Ar using a laser-induced fluorescence technique.

The present research was also stimulated by recent theoretical work of Czuchaj and Stoll [17] who performed *ab initio* calculations of potential energy curves for Cd-Rare gas systems, as well as by recent experimental studies of Cd–Ar excimers created in free supersonic expansion

[a] e-mail: rst@phys.uni.torun.pl

[18] in which spectroscopic constants for CdAr molecule were determined assuming the Morse potential.

2 Experimental setup

In order to avoid the hyperfine and isotopic structure of the Cd 326.1 nm line we used the ^{114}Cd isotope. The side-arm quartz cells containing cadmium were filled with argon and cut-off from the vacuum system. The argon pressure was varied between 5 and 434 torr at room temperature. The cells were situated in the special multisection oven enabling the independent temperature stabilization of the cell and its side-arm up to 1 K. During the measurement the temperature of the cell was kept constant at 724 K, while the side-arm was kept at temperature 440 K.

The line shape of the cadmium 326.1 nm line was registered using a digital laser spectrometer described elsewhere [19]. An actively stabilized single-frequency Coherent CR 899-21 ring dye laser equipped with intracavity frequency doubler, operating on DCM dye was pumped by INNOVA–400 argon-ion laser. The ring laser provided single mode UV output continuously tunable for up to 60 GHz with a line width of about 1 MHz. The intensity of the fluorescence signal was measured by a thermoelectrically cooled photomultiplier working in the photon counting mode. Frequency calibration of the ring laser was performed using its fundamental (red) line directed to a confocal Fabry-Perot interferometer (FPI) with a free spectral range of 1.5 GHz and the 100 cm long iodine cell operated at temperature 35 °C. The FPI transmission peaks and I_2 absorption spectrum were recorded simultaneously with the fluorescence signal for frequency calibration. The laser UV beam incident on the cell was linearly polarized in the vertical direction and the collection optics arm, perpendicular to the laser beam direction, contained a linear polarizer set at the "magic angle" (rotated 54.7° from the vertical), so the collection optics system was insensitive to effects due to anisotropy of fluorescence (see *e.g.* [20,21]). Photon counting was performed by an electronic system built in the CAMAC standard described elsewhere [15]. All the data: fluorescence signal, laser UV output power, FPI transmission peaks and I_2 absorption spectrum were acquired with a PC computer for further evaluation.

3 Line shape

In the traditional analysis of line shapes one assumes that the Doppler broadening is statistically independent of pressure broadening. In the impact limit the combined influence of Doppler and pressure effects can be represented by the familiar Voigt profile $I_{\mathrm{VP}}(\widetilde{\nu})$ which is a convolution of the Lorentzian and Gaussian profiles. Beyond the impact limit, *i.e.* in the case when the finite duration of collisions is taken into account the resultant profile can be represented by the so-called asymmetric Voigt profile $I_{\mathrm{AVP}}(\widetilde{\nu})$ which is a convolution of the collisional $I_{\mathrm{C}}(\widetilde{\nu})$ and Doppler $I_{\mathrm{D}}(\widetilde{\nu})$ components

$$I_{\mathrm{AVP}}(\widetilde{\nu}) = I_{\mathrm{C}}(\widetilde{\nu}) \otimes I_{\mathrm{D}}(\widetilde{\nu}). \tag{1}$$

The collisional component of the line profile $I_{\mathrm{C}}(\widetilde{\nu})$ can be presented as a sum of the Lorentzian and dispersion profiles [3,6]

$$I_{\mathrm{C}}(\widetilde{\nu}) = I_{\mathrm{C}}^{(0)} \left(\frac{\gamma_{\mathrm{L}}}{2}\right) \frac{(\gamma_{\mathrm{L}}/2) + \chi(\widetilde{\nu} - \widetilde{\nu}_0 - \Delta)}{(\widetilde{\nu} - \widetilde{\nu}_0 - \Delta)^2 + (\gamma_{\mathrm{L}}/2)^2}\cdot \tag{2}$$

Here γ_{L}, Δ and χ denote the Lorentzian width (FWHM), pressure shift, and collision-time asymmetry parameter, respectively, $I_{\mathrm{C}}^{(0)}$ is the intensity in the line peak and $\widetilde{\nu}_0$ is the unperturbed wavenumber of the emitted line.

The Doppler component $I_{\mathrm{D}}(\widetilde{\nu})$ of the line profile is given by the formula

$$I_{\mathrm{D}}(\widetilde{\nu}) = \frac{2\sqrt{\ln 2}}{\gamma_{\mathrm{D}}\sqrt{\pi}} \exp\left[-\frac{4\ln 2}{\gamma_{\mathrm{D}}^2}(\widetilde{\nu} - \widetilde{\nu}_0)^2\right], \tag{3}$$

where γ_{D} is the Doppler (FWHM) width of the line.

The Lorentzian width and shift can be evaluated from the following expression [1,2,22]:

$$\frac{\gamma_{\mathrm{L}}}{2} + \mathrm{i}\Delta = \frac{N}{c}\int \mathrm{d}^3\mathbf{v} f(\mathbf{v})\, v \int_0^{+\infty} \mathrm{d}\rho\, \rho \times \left\{1 - \left\langle S_{ii}(\rho, v) S_{ff}^{-1}(\rho, v)\right\rangle_{\mathrm{Ang.Av.}}\right\}\cdot \tag{4}$$

Here N is the perturber density, ρ is the impact parameter, $f(\mathbf{v})$ is the Maxwellian distribution of the relative velocities $\mathbf{v}$ of the colliding atoms and $S_{ii}(\rho, v)$ and $S_{ff}(\rho, v)$ are the diagonal elements of the scattering matrix $\widehat{S} = \widehat{U}(-\infty, +\infty)$ for the initial and final states of the radiating atom expressed as functions of ρ and v. Here $\widehat{U}(t_2, t_1)$ denotes the time evolution operator and the symbol $\left\langle S_{ii} S_{ff}^{-1}\right\rangle_{\mathrm{Ang.Av.}}$ means the average over angular coordinates.

The collision-time asymmetry parameter can be evaluated from the expression derived in papers [10,22]:

$$\begin{aligned}\chi = 2\pi N \int \mathrm{d}^3\mathbf{v} f(\mathbf{v})\, v \int_0^{+\infty} \mathrm{d}\rho\, \rho \\ \times \int_{-\infty}^{+\infty} \mathrm{d}t_0\, \mathrm{Im}\{1 + \langle U_{ii}(+\infty, -\infty) U_{ff}^{-1}(+\infty, -\infty) \\ - U_{ii}(t_0, -\infty) U_{ff}^{-1}(t_0, -\infty) \\ - U_{ii}(+\infty, t_0) U_{ff}^{-1}(+\infty, t_0)\rangle_{\mathrm{Ang.Av.}}\}.\end{aligned} \tag{5}$$

In order to adapt the above approach to the analysis of experimental line shapes for the Cd–Ar system, the interatomic potentials involving the Cd ground ($5s^2\ ^1\mathrm{S}_0$) and the excited ($5s5p\ ^3\mathrm{P}_1$) states must first be known. The interaction between the ground state atoms $\mathrm{Cd}(5s^2\ ^1\mathrm{S}_0) + \mathrm{Ar}(3p^6\ ^1\mathrm{S}_0)$ is described by a single potential curve corresponding to the $X^1 0^+$ molecular state. During the collision of the Cd atom excited to

the $5s5p\,^3\mathrm{P}_1$ state two molecular states labeled as A^30^+ and B^31 are formed which are described by two different potential curves. The broadening and shift of the Cd 326.1 nm intercombination line ($5s5p\,^3\mathrm{P}_1$–$5s^2\,^1\mathrm{S}_0$) is thus the result of contributions from the A^30^+–X^10^+ and B^31–X^10^+ transitions. In the adiabatic approximation for the Cd 326.1 nm line perturbed by Ar the product of time-evolution operators averaged over angular coordinates can be written as [10,14]:

$$\left\langle U_{ii}(t_2,t_1)U_{ff}^{-1}(t_2,t_1)\right\rangle_{\mathrm{Ang.Av.}} = \frac{1}{3}\exp[-\mathrm{i}\eta_{A-X}(t_2,t_1)] + \frac{2}{3}\exp[-\mathrm{i}\eta_{B-X}(t_2,t_1)], \quad (6)$$

where $\eta_{A-X}(t_2,t_1)$ and $\eta_{B-X}(t_2,t_1)$ are the phase-shifts for the A^30^+–X^10^+ and B^31–X^10^+ transitions, respectively. These phase-shifts are given by the following expression:

$$\eta(t_2,t_1) = \frac{1}{\hbar}\int_{t_2}^{t_1} \Delta V(r(\tau))\mathrm{d}\tau, \quad (7)$$

where $\Delta V(r)$ denotes the difference of potentials $V(A^30^+)$ – $V(X^10^+)$ (or $V(B^31)$ – $V(X^10^+)$) and $r(\tau) = \sqrt{\rho^2 + v_{\mathrm{EP}}^2\tau^2}$ is the interatomic distance at time τ.

4 Data analysis

The assumption of statistical independence of the Doppler broadening from the pressure effects is justified only in the case when the mass of the emitter m_{E} is greater than that m_{P} of the perturber. For systems corresponding to small values of $\alpha = m_{\mathrm{P}}/m_{\mathrm{E}}$, the ratio of perturber and emitter masses, the emitters are essentially stationary and all collisions are independent of the emitter velocity $\mathbf{v}_{\mathrm{E}}$ so that either $I_{\mathrm{AVP}}(\widetilde{\nu})$ or $I_{\mathrm{VP}}(\widetilde{\nu})$ are applicable depending on whether the finite duration time of collisions is, respectively, taken into account or not.

For the Cd–Ar system the ratio of perturber to emitter mass is equal to 0.35 which means that the Doppler-collision correlation should not play any essential role. Therefore in order to examine the influence of the collision-time asymmetry on the total line shape we fitted two profiles to our experimental data: ordinary Voigt profile $I_{\mathrm{VP}}(\widetilde{\nu})$ and asymmetric Voigt profile $I_{\mathrm{AVP}}(\widetilde{\nu})$. The best fit procedure was performed using a least-squares algorithm for nonlinear parameters due to Marquardt [23]. Our numerical fit to $I_{\mathrm{VP}}(\widetilde{\nu})$ allowed three parameters to vary: the Gaussian width γ_{D}, the Lorentzian width γ_{L} and the line shift Δ. For asymmetric $I_{\mathrm{AVP}}(\widetilde{\nu})$ profile we also fitted the asymmetry parameter χ.

Figure 1A shows an example of the shape of the 326.1 nm ^{114}Cd line perturbed by Ar at 251 torr at room temperature. The best fit profile $I_{\mathrm{AVP}}(\widetilde{\nu})$ is plotted as the solid line. In order to examine the quality of the fits we used the weighted differences of the intensities

$$D_\sigma(\widetilde{\nu}) = \frac{I_{\mathrm{exp}}(\widetilde{\nu}) - I_{\mathrm{theor}}(\widetilde{\nu})}{\sqrt{I_{\mathrm{theor}}(\widetilde{\nu})}}, \quad (8)$$

between experimental (measured) $I_{\mathrm{exp}}(\widetilde{\nu})$ and theoretical (fitted) $I_{\mathrm{theor}}(\widetilde{\nu})$ profiles. In Figure 1B we plotted these differences for the case when $I_{\mathrm{theor}}(\widetilde{\nu})$ profile was given by the ordinary Voigt profile $I_{\mathrm{VP}}(\widetilde{\nu})$. We can see systematic departures from zero in the line core as well as on line wings which can be regarded as a manifestation of the line asymmetry.

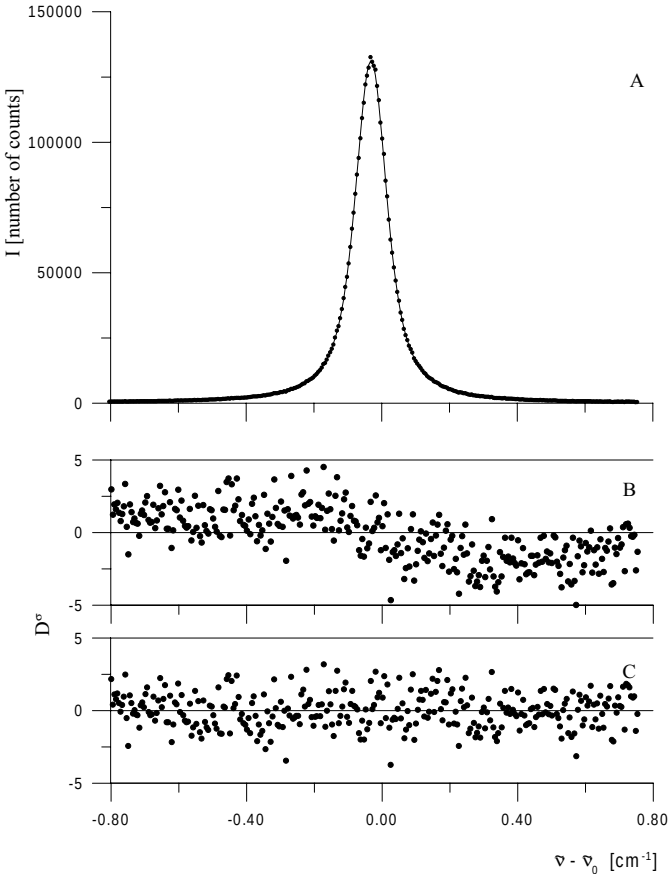

Fig. 1. The shape of the Cd 326.1 nm line perturbed by argon at pressure 251 torr; (A) experimental points together with the best-fit AVP (full curve), (B) and (C) weighted differences $D_\sigma(\widetilde{\nu})$ between experimental and fitted VP and AVP profiles, respectively.

Figure 1C shows the differences for the case when $I_{\mathrm{theor}}(\widetilde{\nu})$ is given by the asymmetric Voigt profile $I_{\mathrm{AVP}}(\widetilde{\nu})$. As can be seen in this case the values of the differences are spread uniformly about zero which confirms the quality of the fit. We can thus conclude that in the case of the Cd–Ar system the collision-time asymmetry has a noticeable influence on the profile of the 326.1 nm line.

Figure 2 shows the values of the Doppler width γ_{D} of the 326.1 nm Cd line perturbed by argon determined from the best fit of the AVP to the experimental data, plotted against the pressure of Ar. As can be seen there is practically no dependence of the Doppler width γ_{D} on the Ar-pressure. It confirms the statistical independence between pressure and Doppler broadening for the Cd–Ar system. The average Doppler width is found to be $54.8(2.7) \times 10^{-3}$ cm^{-1}. This value agrees very well with theoretical Doppler width 55.4×10^{-3} cm^{-1} corresponding to the cell temperature $T = 724$ K.

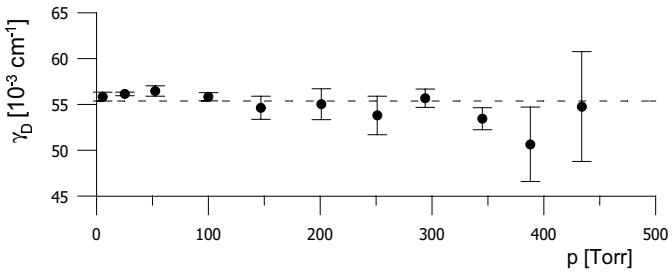

Fig. 2. Plot of the Doppler width $\gamma_{\rm D}$ of the 326.1 nm Cd line perturbed by argon against the pressure of Ar. The widths $\gamma_{\rm D}$ are determined from the best fit of the AVP to the experimental data. Dashed line – Doppler width calculated from the cell temperature (724 K). Error bars indicate the value of the standard deviation.

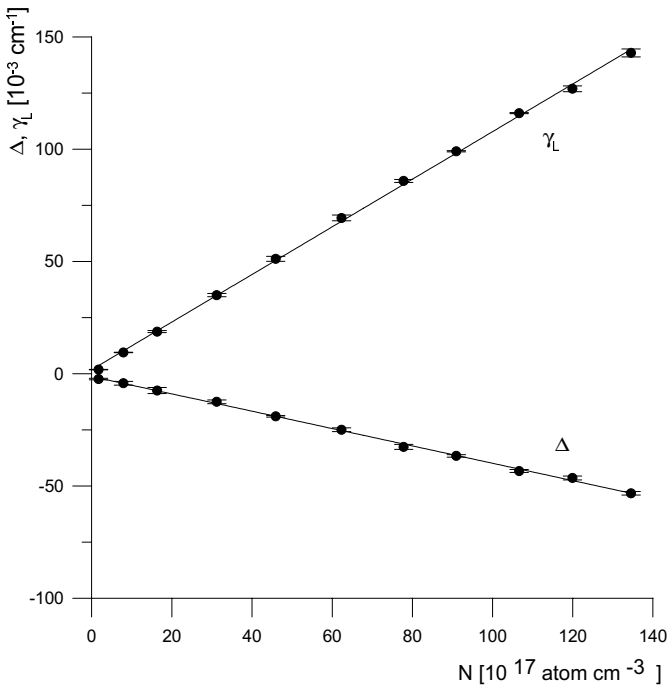

Fig. 3. Plot of the Lorentzian width $\gamma_{\rm L}$ and shift Δ of the 326.1 nm Cd line determined from the best fit of the AVP to the experimental data against the argon density N. Error bars indicate the value of the standard deviation.

Figure 3 shows the plots of the Lorentzian width $\gamma_{\rm L}$ and shift Δ determined from the best fit of $I_{\rm AVP}(\widetilde{\nu})$ to our experimental profiles against the density number N of argon. As it is seen the shift is towards the red and both $\gamma_{\rm L}$ and Δ are linearly dependent on the density. From the slopes of these linear dependencies the pressure broadening $\beta = \gamma_{\rm L}/N$ and shift $\delta = \Delta/N$ coefficients were determined and listed in Table 1.

Figure 4 shows the plot of the asymmetry parameter χ determined from the best fit of $I_{\rm AVP}(\widetilde{\nu})$ to our experimental profiles, against the density number N. As it is seen the asymmetry parameter is linearly dependent on the density. From the slope of the best fit straight line the asymmetry coefficients $\kappa = \chi/N$ were determined and listed in Table 1.

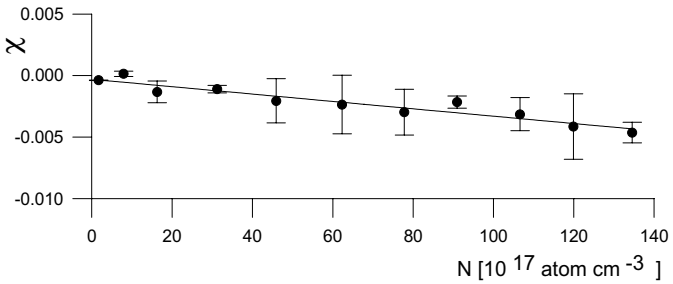

Fig. 4. Plot of the asymmetry parameter χ determined from the best fit of AVP to the experimental data against the argon density N. Error bars indicate the value of the standard deviation.

Table 1. Comparison of experimental values of the β, δ (in units 10^{-20} cm^{-1}/atom cm^{-3}) and κ (in units 10^{-21}/atom cm^{-3}) coefficients with those calculated for different interatomic potentials. For experimental data the values of standard deviations are given.

Experimental values	$\beta_{\rm exp}$	$\delta_{\rm exp}$	$\kappa_{\rm exp}$
This work	1.060(6)	−0.387(4)	−0.30(5)
Brym *et al.* [16]	1.04(2)	−0.29(3)	—
Dietz *et al.* [13]	0.94(16)	−0.43(20)	—
Theoretical values	$\beta_{\rm theor}$	$\delta_{\rm theor}$	$\kappa_{\rm theor}$
Czuchaj-Stoll [17]	1.334	−0.358	−0.85
Morse	1.439	−0.204	−0.70
Lennard-Jones	0.940	−0.291	−0.37
van der Waals	0.964	−0.350	−0.55

5 Results and discussion

We have shown that the AVP, equation (1), gives a correct description of our experimental profiles of the ^{114}Cd 326.1 nm line perturbed by argon.

The experimental values of pressure broadening β, shift δ and asymmetry κ coefficients determined in the course of the present work are listed in Table 1. In a previous work [16] from this laboratory the β and δ coefficients for the 326.1 nm Cd line perturbed by Ar were determined using a classical spectroscopy technique, *i.e.* by means of a pressure scanned Fabry-Perot interferometer for the cell temperature $T = 468$ K. These values are listed in Table 1 where they are marked "Brym *et al.* [16]". In Table 1 we have also listed the experimental values of the broadening and shift coefficients determined by Dietz *et al.* [13] from the Cd 326.1 nm line shape measurements performed in the temperature range between 503 K and 663 K, (marked "Dietz *et al.* [13]").

As it can be seen from Table 1 there is a good agreement between the values of β and δ coefficients determined from three different experiments performed for different temperatures. Our two independent experiments confirm Dietz *et al.* [13] observation that for the 326.1 nm Cd line perturbed by Ar the line shape parameters are independent of the temperature.

Measurements of pressure broadening β, shift δ and asymmetry κ coefficients performed in the present study

enabled us to verify known interaction potentials for the Cd–Ar system. In order to do this we calculated the theoretical values of pressure broadening β and shift δ coefficients from equation (4) for different interaction potentials. We performed the calculation for the Czuchaj and Stoll [17] numerical potential as well as for two potentials derived from experimental data *i.e.* for Morse and Lennard-Jones potentials with the same spectroscopic constants for the A^30^+ state as used in reference [16], and new values of these constants determined recently for B^31 and X^10^+ states by Koperski *et al.* [18]. We also calculated the values of β and shift δ coefficients assuming the interaction potential in the van der Waals form, using the same values of C_6 force constants calculated in Coulomb approximation as used in our earlier work [16].

The values of β and δ coefficients evaluated for these potentials are listed in Table 1 and marked as "Czuchaj-Stoll [17]", "Morse", "Lennard-Jones" and "van der Waals", respectively. As can be seen from Table 1 there is generally poor agreement between the experimental and theoretical values both for β and δ coefficients. Our experimental value of β coefficient is closest to theoretical value obtained for the van der Waals and Lennard-Jones potential.

The experimental values of collision-time asymmetry coefficients κ determined in the course of the present work are listed in Table 1 where they are compared with theoretical values. We have shown recently [12] that in the case of the van der Waals potential the values of the asymmetry parameter calculated in the framework of the unified Franck-Condon treatment [3,6] are very close to that obtained from formula (5) corresponding to the Anderson-Talman approach [4,5]. It should be noted, however, that equation (5) is more convenient for numerical application, especially in averaging over Maxwellian distribution of velocities than other known expressions [6,7]. Therefore theoretical values of asymmetry coefficient κ were calculated from equation (5) for the Czuchaj and Stoll [17] numerical potential as well as for Morse, Lennard-Jones and van der Waals potentials. As can be seen from Table 1 good agreement between our experimental and theoretical values of the asymmetry coefficient κ takes place for the Lennard-Jones potential.

6 Conclusion

The comparison of pressure broadening, shift and asymmetry coefficients determined in this experiment with coefficients calculated on the basis of the adiabatic semiclassical approach shows poor agreement between experimental and theoretical values obtained for numerical potentials calculated by Czuchaj and Stoll [17] as well as for potentials derived from experimental data *i.e.* for Morse and Lennard-Jones potentials. It should be noted, however, that in the case of the Czuchaj-Stoll potential the theoretical value of the pressure shift coefficient δ is much closer to the experimental value than that of the broadening coefficient. On the other hand, the theoretical value of δ calculated from the Czuchaj-Stoll potential agrees well with that corresponding to the van der Waals potential. Contrary to that, theoretical value of the pressure broadening coefficient calculated from the Czuchaj-Stoll potential differs from that obtained from the van der Waals interaction. We can thus conclude that new calculations of the interatomic potentials for Cd–Ar are necessary to explain the experimental data on the broadening, shift and asymmetry of the Cd intercombinational line shape.

The authors wish to express their gratitude to Professor E. Czuchaj for making available numerical values of potentials and to Professor J. Szudy for valuable help in the preparation of the manuscript. This work was supported by a grant No. 673/PO3/96/10 (2 PO3B 005 10) from the State Committee for Scientific Research.

References

1. M. Baranger, Phys. Rev. **111**, 494 (1958).
2. N. Allard, J. Kielkopf, Rev. Mod. Phys. **54**, 1103 (1982).
3. J. Szudy, W.E. Baylis, Phys. Rep. **266**, 127 (1996).
4. P.W. Anderson, J.D. Talman, *Conference on Broadening of Spectral Lines*, University of Pittsburg, unpublished (1955); *Bell Teleph. Syst. Tech. Publ.* No. 3117.
5. G. Traving, *Uber die Theorie der Druckverbreiterung von Spektrallinien* (Verlag G. Braun, Kalsruhe, 1960).
6. J. Szudy, W.E. Baylis, J. Quant. Spectrosc. Radiat. Transf. **15**, 641 (1975); *ibid.* **17**, 681 (1977).
7. A. Royer, Acta Phys. Pol. A **54**, 805 (1978).
8. B.N.I. Al-Saqabi, G. Peach, J. Phys. B **20**, 1175 (1987).
9. P.S. Julienne, F.H. Mies, Phys. Rev. A **34**, 3792 (1986).
10. R. Ciuryło, J. Szudy, R.S. Trawiński, J. Quant. Spectrosc. Radiat. Transf. **57**, 551 (1997).
11. J. Domysławska, A. Bielski, R.S. Trawiński, J. Quant. Spectrosc. Radiat. Transf. **61**, 735 (1999).
12. A. Bielski, R. Ciuryło, J. Domysławska, D. Lisak, R.S. Trawiński, J. Szudy, Phys. Rev. A **62**, 032511 (2000).
13. K.J. Dietz, P. Dabkiewicz, H.J. Kluge, T. Kühl, H.A. Schuessler, J. Phys. B **13**, 2749 (1980).
14. S. Brym, R. Ciuryło, R.S. Trawiński, A. Bielski, Phys. Rev. A **56**, 4501 (1997).
15. A. Bielski, S. Brym, R. Ciuryło, J. Domysławska, E. Lisicki, R.S. Trawiński, J. Phys. B **27**, 5863 (1994).
16. S. Brym, R. Ciuryło, E. Lisicki, R.S. Trawiński, Phys. Scripta **56**, 541 (1996).
17. E. Czuchaj, H. Stoll, Chem. Phys. **248**, 1 (1999).
18. J. Koperski, Sz. M. Kiełbasa, M. Czajkowski, Spectrochim. Acta A **56**, 1613 (2000).
19. A. Bielski, R. Ciuryło, J. Domysławska, D. Lisak, R.S. Trawiński, J. Wolnikowski, Acta Phys. Pol. A **97**, 1003 (2000).
20. M. Harris, E.L. Lewis, D. McHugh, I. Shannon, J. Phys. B **19**, 3207 (1986).
21. R.E. Walkup, A. Spielfiedel, D. Ely, W.D. Phillips, D.E. Pritchard, J. Phys. B **14**, 1953 (1981).
22. R. Ciuryło, Phys. Rev. A **58**, 1029 (1998).
23. D.W. Marquardt, J. Soc. Industr. Appl. Math. **11**, 431 (1963).